Adaptive Solar Home Systems

Eric Thorne
Dr. Gary Ybarra
Grant Means
Duke University Department of Electrical and Computer Engineering
NAE Grand Challenges Scholars Program

April 29, 2011

Acknowledgements

I thank Drs. Ybarra and George for helping me debug the circuit. I also thank Kip Coonley and Justin Miles for always helping me track down the parts I needed. Deans Katsouleas, Absher, and Dr. Reichert: thank you for your commitment to the GCSP program. I had a great time with this research and am certain that I will use what I have learned in the future. Will Patrick and Jas Garcha: if it weren't for you all, then I wouldn't have had the chance to work with Village Energy. Finally, to Roey, Mary, and Abu: I will not forget my Ugandan family, ever.

Here's to staying idealistic.

Contents

1 Abstract

The approximately linear correlation between per capita electricity use and HDI motivates a particular approach for rapidly improving worldwide quality of life while removing dependence on nonrenewable sources of energy. We present a modular and adaptable system design for decentralized solar home systems. The system incorporates battery protection through the use of low- and high-voltage cutoffs, and a maximum power point tracker to continuously extract the maximum power from the solar panel at all times. We worked with a real solar power startup, Village Energy, which has a unique business model that we believe positions it to serve a very large market. We are also working with the North Carolina School of Science and Math to implement a solar educational program. These steps progress towards the transition to an economical solar solution for energy needs wordwide.

2 Introduction

2.1 The Grand Challenge of solar power

Sunlight is a clean, renewable, and abundant source of energy that has the potential to power the entire world. Over the course of the year in 2008, the entire world used 15 TW while the Sun radiated approximately 174 PW to Earth's upper atmosphere in the same timeframe [1,2]. Efficient collection, storage and distribution of this ten-thousandfold source of power would solve many of the world's most pressing problems, including electricity access, pollution and contamination from fossil fuels and nuclear technologies, and energy politics. Unfortunately, current solar energy technologies are infamously inefficient. Current commercially available photovoltaic cells have an efficiency ceiling of only 31 percent [3].

It is not surprising, then, to see much time and money going into research and development of this area. In 2008, at the behest of the US Government, the National Academy of Engineering (NAE) announced fourteen "Grand Challenges of Engineering", one of which is "Make Solar Energy Economical". The announcement aimed to re-create the affects of the Sputnik launch in 1957, focusing research efforts and creating new value for math, science, and engineering educational programs. To support this effort at the collegiate level, partner institutions Duke, Olin, and Southern California co-founded the Grand Challenges Scholars program.

This research project is in partial fulfillment of the Grand Challenges Scholars distinction. In addition to an in-depth research component, the program also requires demonstrated interdisciplinary curricular work, entrepreneurship, global perspective, and service learning. For more information about this integration, please see the "Thematic Coherence" section.

2.2 Measuring success through effective diffusion

Since the goal of the target Grand Challenge is to make solar energy "economical", we decided to quantify "economical" by breaking it into distinct metrics. Metrics are useful in making design decisions and reflecting on success because they define a weighted value system. For example, when choosing between two lighting systems, the most heavily weighted metrics might include brightness and reduction of eyestrain. The lighting system that is the brightest and reduces eyestrain the most will probably be selected. For our purposes we used (1).

$$\text{“}economical\text{”} = access + scale + effects + compatibility \tag{1}$$

We will now describe each of the terms in the equation.

"Access" describes how easily a potential user is able to obtain and use our product. It includes price, difficulty of acquisition, installation or use, and physical compatibility. For example, an appliance that works only on 50 VAC, 100 Hz is not very "accessible" because no power outlets in the world provide this power.

"Scale" describes how deeply our product can penetrate a market and how easily it can enter into new markets. Is it compatible across large regions of the world? Returning to the wall socket example, it is apparent that appliances should be designed to be compatible with the power outlets of the entire clientele, or be easily adapted to those outlets.

"Effects" describes the long- and short-term effects of our product. Does it create pollution? Does the packaging create a lot of waste? Kerosene lamps are a viable solution to the lighting problem in many developing countries, but they are also responsible for fires that cause loss of property and, in some cases, loss of life.

"Compatibility" describes the amount of resistance that our product will have in being adopted by users due to social and cultural factors. E.M. Schumacher illustrates the role of social and cultural networks in product adoption in *Elements of Diffusion*. He describes a case study in which Nelida, a social worker from a metropolitan area of Peru, attempts to persuade rural villagers in another part of the country to adopt water boiling for improved health.

Nelida visited homes in the village and attempted to explain the benefits of boiling water with germ theory. After two years of working with over 200 families, she was only able to persuade about five percent of the population, eleven families, to adopt. This was because water boiling was perceived as culturally unacceptable in the community. For example, one rejecter explained that "cooked" foods and drinks such as boiled water were traditionally reserved for the ill. Another rejecter, unable to grasp the concept of life forms so small that they could not be seen, did not understand Nelida's germ theory explanation. One adopter, however, was notably removed from the mainstream social and cultural channels due to having recently moved to the village from another part of the country.

These examples show that diffusion of new technologies is a phenomenon of human communication over time [4]. If Nelida had been conscious of the belief system in the community, then she could have made her explanation of water boiling more appealing to families. She also could have tapped into the social system inside the community. Like the adopter in the last example, Nelida was no doubt perceived by indigenous villagers as an outsider. A respected member of the community that can be trusted and related to would be more persuasive.

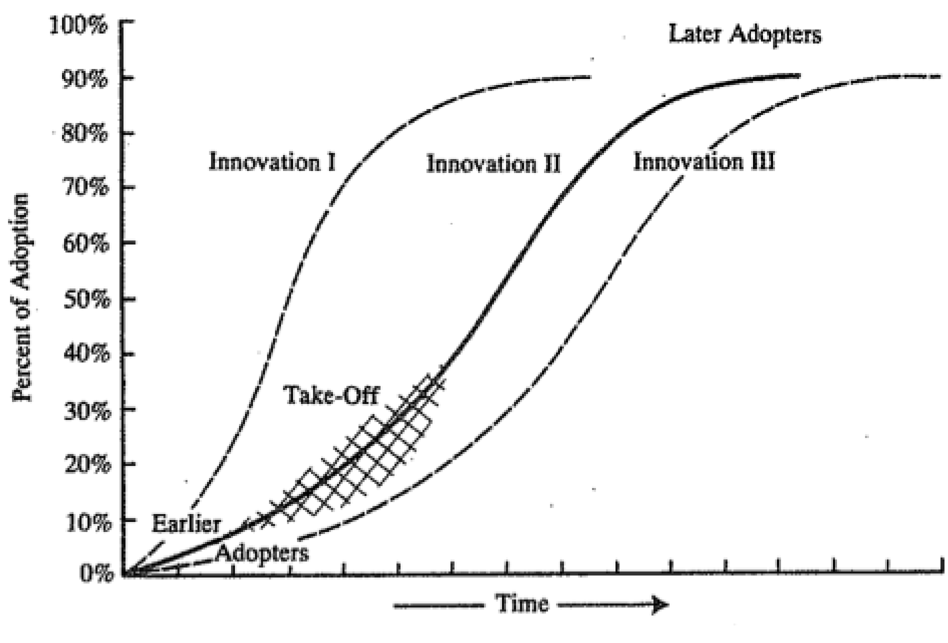

Figure 1: Illustration of the diffusion process. Note the point of widespread adoption that occurs after the Take-Off zone.

The process of diffusion can be visualized in Fig. 1. At first only early adopters will use the product - these people may have prior experience, or are savvier in general. Gradually (if a product is successful) more and more users will adopt until a critical mass is reached (the Take-Off zone). Once this point is reached, the product will have enough exposure in enough social networks to be quickly and widely adopted by most potential users.

Economy and diffusion, as they have been defined here, work together for the successful deployment of a product. Economy is the design-centric side and diffusion is the execution-centric side of the same coin. After describing these metrics we could then evaluate several potential approaches in solving the Grand Challenge.

3 Motivation and approach

The approach that we determined to be the most promising in solving the Grand Challenge enfranchises the largest number of people with basic electricity through the efficient use of more and more inexpensive solar hardware. The target market is the currently electricity-disenfranchised: those living without grid access who use the light of kerosene, if at all, to see at night.

We arrived at this conclusion by compiling a table of alternatives (see Table I) and using (1) with the following weights: access, scale, and compatibility are equally important and so get an equal weight of 2, and effects is less important so gets a weight of 1. Scoring is as follows: each design is ranked against every other in each metric category (the higher the better). The sum of the ranks multiplied by the category weight is the final score.

Table I: Trade study of solar proliferation methods

Design/Metric	**Access (2)**	**Scale (2)**	**Effects (1)**	**Compatibility (2)**	**Score**
Increase PV efficiency	1	1	3	3	13
Large package sales	2	3	2	3	18
Small package sales	3	3	2	3	20

Much research goes into the development of more efficient PV technology and the results are promising, with experimental designs at over 50% efficiency [5]. However, these technologies currently do not exist and need time to commercialize before they can be mass-produced and sold at a reasonable price. Therefore PV efficiency research received a lower access and scale score.

Relatively inefficient solar panels are becoming more and more affordable due to their maturity in the product lifecycle. Worldwide manufacturing and competition drive prices down and availability up. Combining several of these cells and leveraging load-side efficiency gains can realize the same output as a more efficient experimental panel at a fraction of the price and at the present time.

Other research advocates for a widespread and relatively "thin", that is, using small-scale systems, deployment of solar PV. Electricity use per capita correlates positively with HDI, a widely used metric for overall quality of life. See Fig. 2. Specifically, GDP per capita (one of the weighted metrics in HDI) versus electricity use per capita has an R^2 of 0.95 [6]. The threshold from moving from a low human development economy to a medium human development economy is around 500 kWh. High human development economies use around 4000 kWh [7].

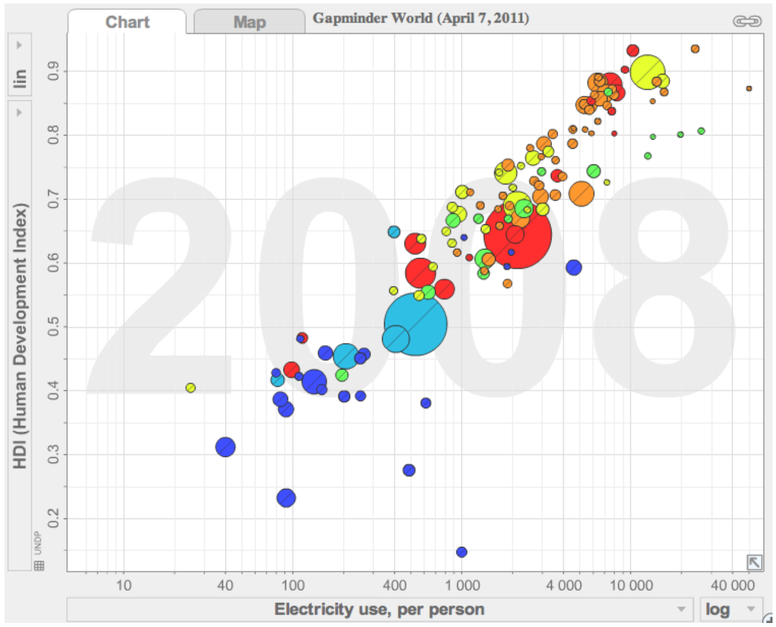

Figure 2: Relationship between per capita electricity use and HDI. Note the approximately linear correlation.

By increasing per-capita electricity use we can accelerate growth, quickly realizing gains in education, productivity, and employment. This creates a positive feedback loop whereby the newly electricity-franchised upgrade their systems and further improve their quality of life and communities.

Our approach is directly derived from these findings.

There are two facets to this strategy: a technical facet and a business facet. The technical facet produced a solar system that is relatively inexpensive but which can quickly and easily be upgraded. The business facet markets and distributes these products over a large population. We have partnered with an indigenous startup company that specializes in solar LED lighting systems, Village Energy (U), Ltd.

4 Technical design

4.1 Overview of solar system

Solar systems are made of three basic parts: a solar panel for collecting energy, a battery for storing energy, and an energy application unit to do useful work with that energy. To increase efficiency and performance, we have added several components. The full system block diagram can be seen in Fig. 3.

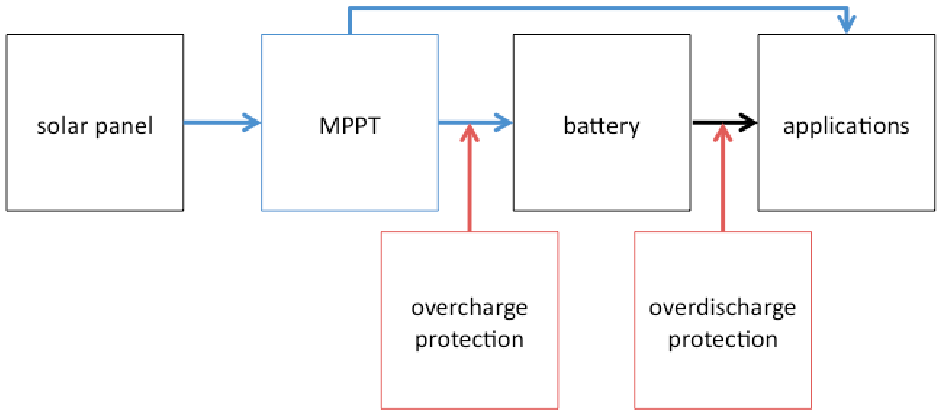

Figure 3: High-level block diagram showing the primary components of solar systems (in black) and the new features that we have added in two design iterations (first iteration is red, second is blue).

4.2 Solar panels

A solar panel has nonlinear voltage-current characteristics. Typical I-V curves for a solar panel are shown in Fig. 4. Note how the I-V curve changes with insolation and temperature, two variables which change constantly throughout the day. Another set of solar I-V curves superimposed with output power curves is shown in Fig. 5. As can be seen in Fig. 5, the maximum power point for any given I-V curve is at the "knee" of the curve. It is this constant changing of the I-V curve, including changes in the maximum power voltage, which will necessitate a maximum power point tracker, discussed later.

4.3 Batteries

All batteries store energy, but the way that they should be charged and discharged depends on the battery chemistry (e.g., Li-ion, NiMH, SLA). If batteries are not used properly, that is, if they are overcharged or overdischarged, then the normal aging process could be accelerated resulting in the inability of the battery to hold any charge.

4.4 Initial system

When researchers partnered with Village Energy, the company already had a working prototype. This solar home system used the most basic design: a solar panel connected directly to a battery pack connected directly to two LED lights. See Figs. 6 and 7 for a picture and the circuit diagram and Tables II and III for descriptions of the parts that were used.

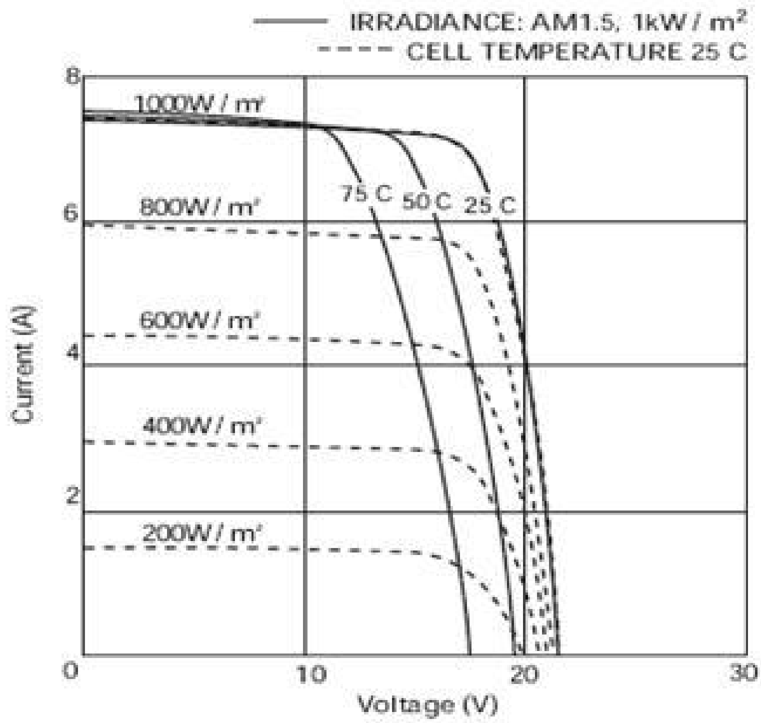

Figure 4: Generalized I-V curves for photovoltaic panels (image credit: alte.com). Note how the I-V curve changes with temperature and insolation.

Table II: 1.5 W solar panel characteristics

Maximum power	1.5 W (7.2 V, 167 mA)
Open circuit voltage	10.5 V
Short circuit current	190 mA

Table III: NiMH battery pack characteristics

Package	3x AA
Nominal cell voltage	1.2 V
Nominal capacity	2300 mAh
Low voltage cutoff	1.0 V

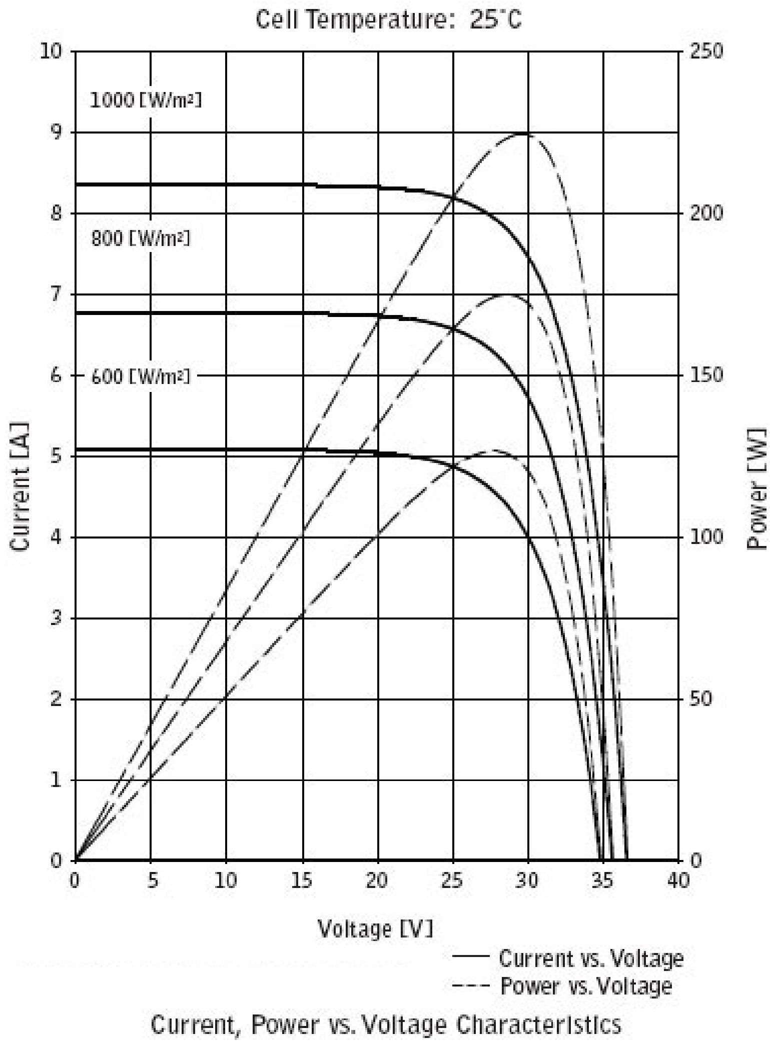

Figure 5: Generalized I-V and power curves for photovoltaic panels (image credit: solarpower-planetearth.com). Note how the I-V curve and the maximum power point change with varying insolation levels and temperature.

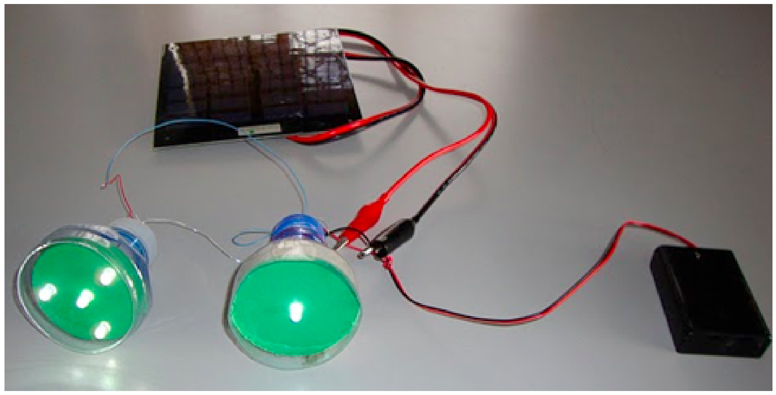

Figure 6: Photo of Village Energy's first solar home lighting system. Note how these lights are meant to be installed from the ceiling, and do not take a lantern form like the lights of most competitors.

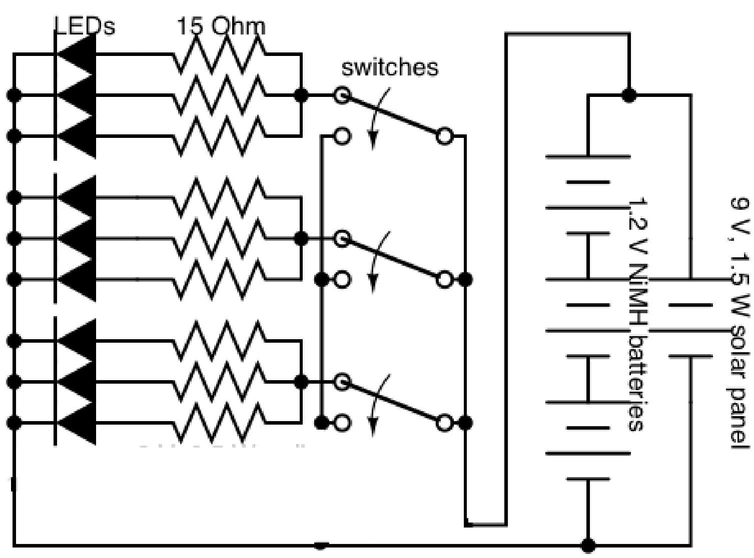

Figure 7: Schematic of Village Energy's first home solar system.

Although this system did work, it had many problems. First, because the solar panel was connected directly to the batteries, it was forced to operate at the battery voltage. This severely limited the power output of the solar panel. The I-V curve of the 1.5 W panel that was used is shown in Fig. 8. The battery pack (3 NiMH cells in series) had a nominal voltage of 3.6 V, so when connected directly to the solar panel it forced operation at the power point indicated by the red arrow. At this power point, the solar panel only generates half of the power generated at the maximum power point, indicated by the blue arrow. This is because the currents at the two power points are about the same, but the voltage at the red arrow is half that at the blue arrow.

The LED load (1 LED per bulb) used about 10.8 W·h per day ($2 \cdot 0.25$ A $\cdot$ 3.6 V $\cdot$ 6 h) and the solar panel under ideal conditions could produce 18 W·h per day (1.5 W $\cdot$ 12 h). However, because the maximum power that could be produced was halved, the solar panel could only transfer at most 9 W·h per day. In reality this amount was less due to nonideality.

This negative daily energy balance caused the battery to slowly lose its charge. Only on days that the lights were not used, which were almost never, could the battery restore some of its charge.

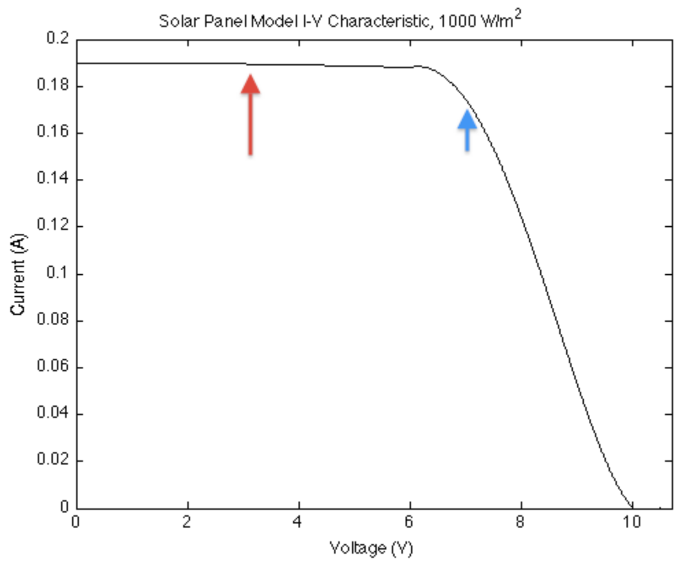

Figure 8: I-V curve of the 1.5 W panel used in Village Energy's first system. The red line indicates the operating point due to the battery pack. The blue line indicates the maximum power point.

The charge balance led to deeper problems because there was no battery protection mechanism. Because the batteries were continuously being discharged past their safe minimum voltage level, they became damaged and their capacity dropped precipitously. Village Energy spent much time and money honoring guarantees by servicing these parts over the first few months of deployment. There was also a risk of overcharge by the solar panel in the case that the application unit was not used for a long time.

Another problem was that the battery voltage was not great enough to properly power the LEDs. White LEDs as used in the system have a forward voltage drop of about 3.2 V. As soon as the battery voltage dropped below 3.2 V, the lights cut out. Coupled with the damaged batteries, this made for many flickering light systems.

Some of the bulbs did not even flicker - they were burnt out. The current control for the LEDs was just a resistor. The voltage dropped across the resistor is proportional to the current by Ohm's Law. Theoretically, if all the resistors were identical then all LEDs would pass the same current. But because the resistors had 5% tolerance, and because of the exponential I-V relationship in a diode, some LEDs used much more current than others. Oftentimes this amount was more than their rated maximum, leading to shorter lifetimes.

One easy way to mitigate this issue is to use 1% tolerance resistors. These resistors are widely available and not very much more expensive. The researchers will advise Village Energy to use these in the next design iteration, but in the future would like to create more sophisticated LED drivers.

4.5 First design iteration

The first phase of this project involved design and fabrication of a fix for these problems that could be inserted into the system as-is. We chose to implement high- and low-voltage cutoffs for battery protection because the battery pack had the lowest per-unit margin on sale and because dead batteries compromised the entire system.

The circuit diagram is shown in Fig. 9, and the PCB layout is shown in Fig. 10.

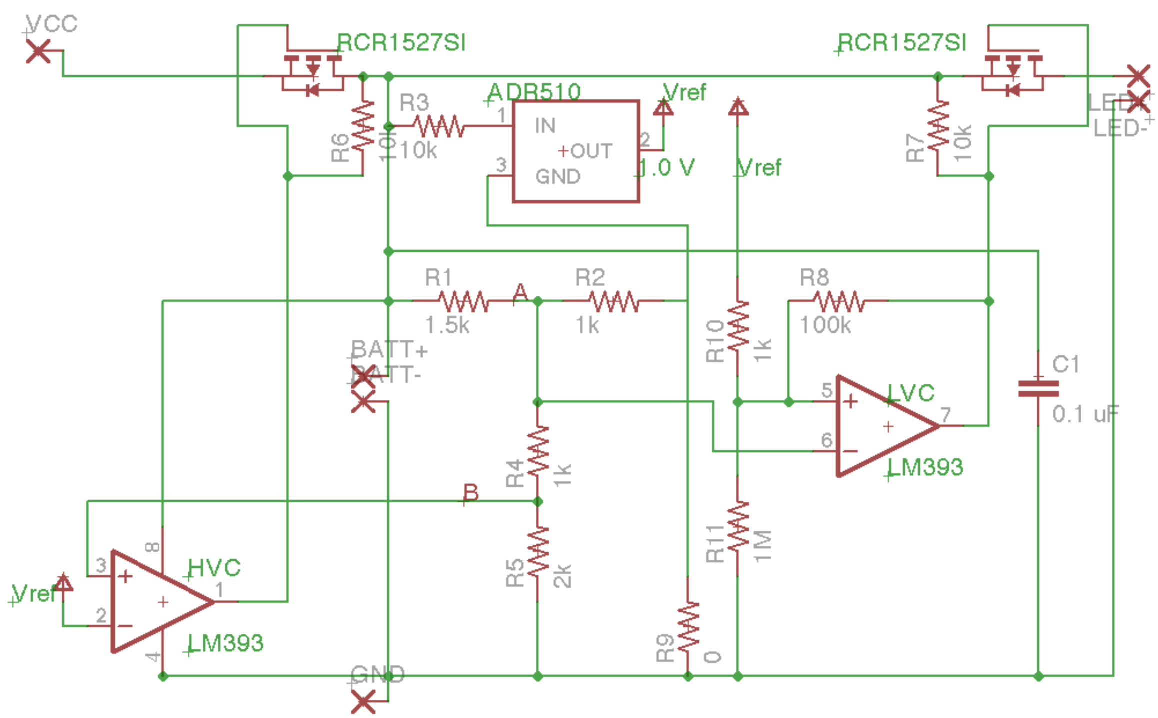

Figure 9: Schematic for first design iteration of Village Energy home system. Incorporates overcharge and overdischarge protection for the battery.

The cutoffs were implemented with a LM393 comparator dual package. The comparators

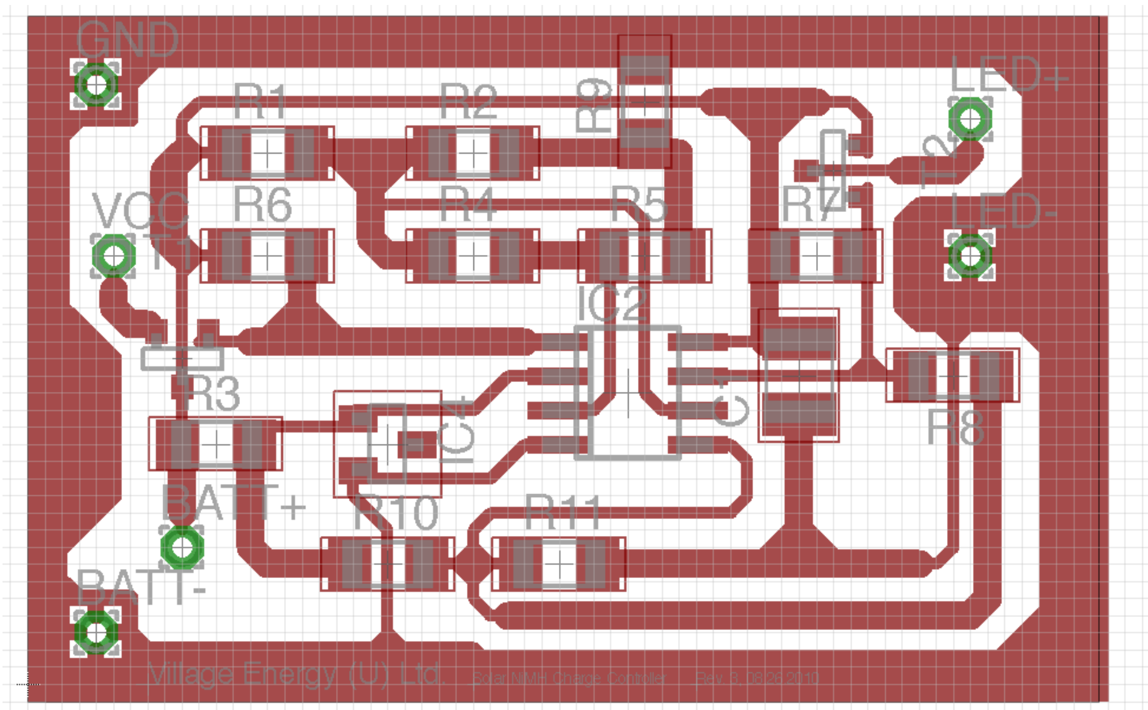

Figure 10: PCB layout for the first design iteration of Village Energy home system.

compared the cell voltage to a set reference that was produced by several voltage divider networks involving an ADR510, which produced a 1.0 V output. The "cell voltage" was the output of a divide-by-3 voltage divider because there was no way to measure each battery from the battery pack. If the batteries are not damaged, then it is fair to assume that they will be at the same state of charge for most of their lifetimes.

Normally the comparators pulled the PMOSFET gates to ground, effectively turning them into short circuits because $V_{gs} < V_{th}$. When either of the comparators detected that the battery needed to be isolated, it would effectively tri-state its output as the LM393 has an open collector output. Pull-up resistors R6 and R7 would then allow a voltage close to the source voltage to appear at the gate, effectively turning the PMOSFET into an open switch.

Hysteresis was also added to the low-voltage cutoff due to the "relaxation" effect of a discharging battery. When it is disconnected from its load, the voltage increases. Without hysteresis, the comparator would think that the battery was charged again, and reconnect it to the load, at which point the voltage would drop below the reference, causing a disconnect and flickering of the lights. Adding about 25 mV of hysteresis prevented switches due to relaxation. Only when the battery was being continuously charged could it be reconnected to the lights. See Fig. 11.

For 2000 units, a manufacturer in China quoted this design at $0.99 per unit. This is a worthy investment considering the relative cost of the battery and the time saved from having to replace them. However, this design still has many problems, first and foremost being the locked operation of the solar panel at the battery voltage.

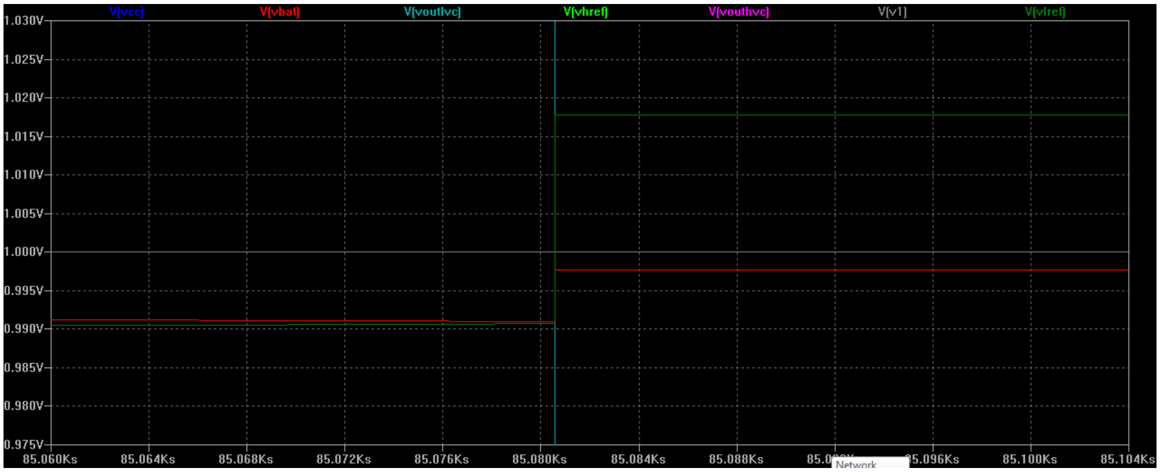

Figure 11: Hysteresis was added to the low-voltage cutoff to debounce the output. Without hysteresis the switch would oscillate.

4.6 Maximum power point tracker

A maximum power point tracker (MPPT) seeks out the solar panel's maximum power output and constrains the circuit to operate at that point. Because the solar panel's I-V curve changes constantly throughout the day due to temperature and insolation flux, this addition can add enormous gains in efficiency. Referring back to Fig. 4, we see that there are distinct I-V curves for different conditions and that the maximum power voltage can decrease.

Our MPPT is built from a buck converter, a microcontroller, and auxiliary circuits to measure current and voltage. See the complete circuit diagram in Fig. 12. We now go into detail about how we designed this system.

4.7 Buck converter

To prevent the solar panel from always being operated at the battery voltage, we must isolate the panel and the battery. Immediately the reader may be reminded of a transformer, which transfers power between two circuits without directly connecting them. The DC analogue of a transformer is a DC-DC converter.

DC-DC converters, specifically, switched DC-DC converters, transform an input voltage to a higher or lower output voltage by selectively storing energy in the electric and magnetic fields of capacitors and inductors. When this energy is released at a different voltage than the input, the current flowing to the output can be modulated. Fig. 13 shows a basic "buck converter" that is used to step down an input voltage to a lower output voltage. This can also be seen in Fig. 12.

We will briefly derive some relationships for the buck converter, but first we need to simplify some of the components. In anticipation of a larger system that could power televisions and refrigerators as well as lights, a 20 W solar panel and 12 V SLA battery were obtained. The solar panel characteristics are summarized in Table IV. Thévenin equivalent sources were derived for each source. A solar panel is not a linear source, but the Thévenin gives us a good understanding

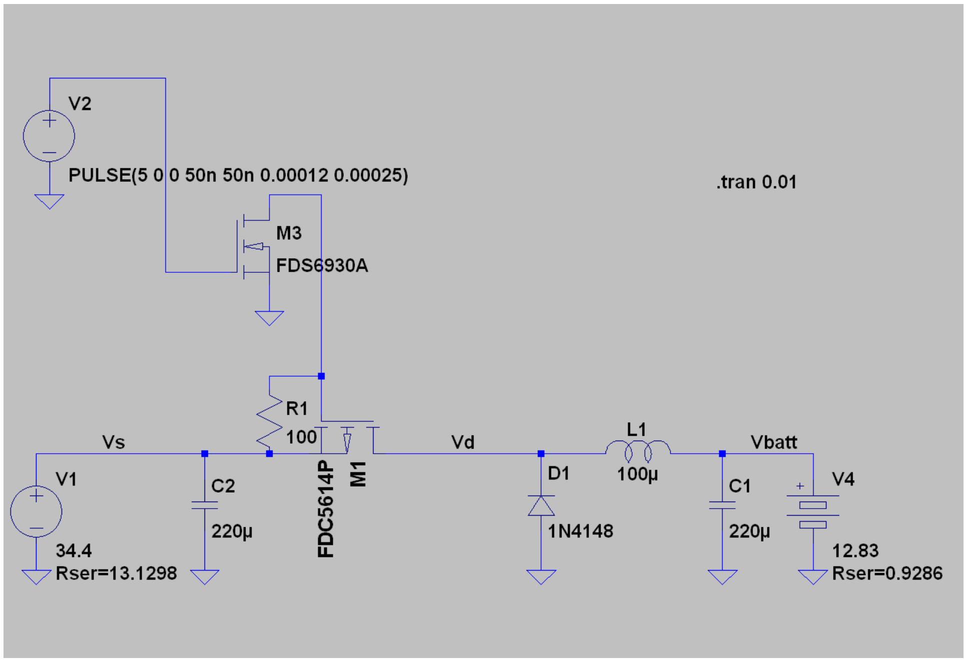

Figure 12: Maximum power point tracker circuit diagram, with comparable models to the actual hardware selected.

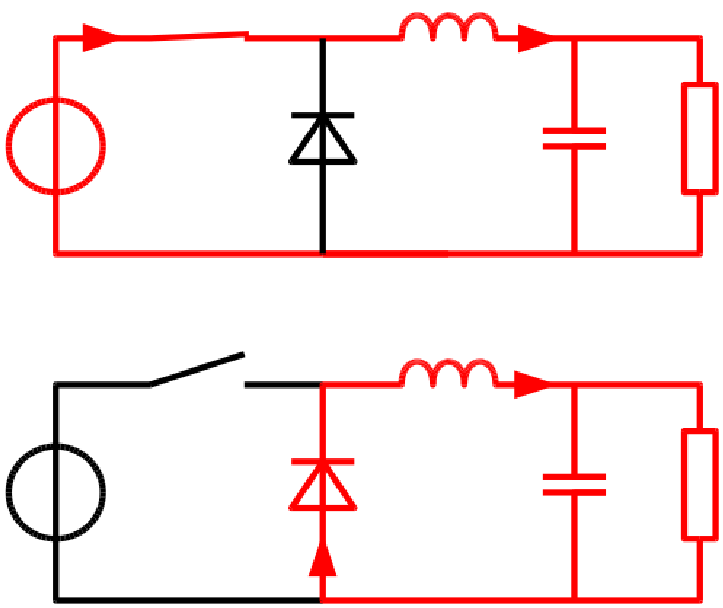

Figure 13: Two states of a basic buck converter.

of what is happening in the circuit.

Table IV: 20 W solar panel characteristics

Maximum power	20 W (17.2 V, 1.13 A)
Open circuit voltage	21.6 V
Short circuit current	1.31 A

Table V: Thévenin equivalents for sources

V_{th}	34.4 V
R_{th}	13.1298 Ω
V_{batt}	12.84 V
R_{batt}	0.9286 Ω

The Thévenin voltage was double the maximum power voltage to ensure that the circuit generated maximum power at the maximum power voltage. A graph of the Thévenin source is shown in Fig. 14.

We will analyze the circuit when the switch is driven with a pulse train with period T_0 and duty cycle D. When switched rapidly, the current will not have time to saturate and so will look like the graphic in Fig. 15; it will remain between two values I_1 and I_2.

When the switch closes, current begins to flow from the voltage source along the outer loop and through the inductor. The current through the inductor begins to rise exponentially and the voltage across it drops at the same rate. The current through the inductor can be calculated from the equation for an exponentially decaying quantity:

$$I(t) = I_f - (I_f - I_i)e^{\frac{-t}{\tau}} \tag{2}$$

Where I_f is the final value that the current will saturate to when the switch is left on for a long time and I_i is the initial value of the current. In the case that the switch is closed, $I_f = I_{max}$ and $I_i = I_2$. By performing Kirchoff's voltage law in each case, we can derive expressions for I_{max} and I_{neg}:

$$I_{max} = \frac{V_{th} - Vbatt}{R_{th} + R_{batt}} \tag{3}$$

$$I_{neg} = \frac{-V_{batt}}{R_{batt}} \tag{4}$$

So we can simplify (2) by substituting $t = DT_0$, taking the first two terms of the Taylor series expansion of the exponential and making the assumption that $DT_0 << \tau = \frac{L}{R_{th}+R_{batt}}$.

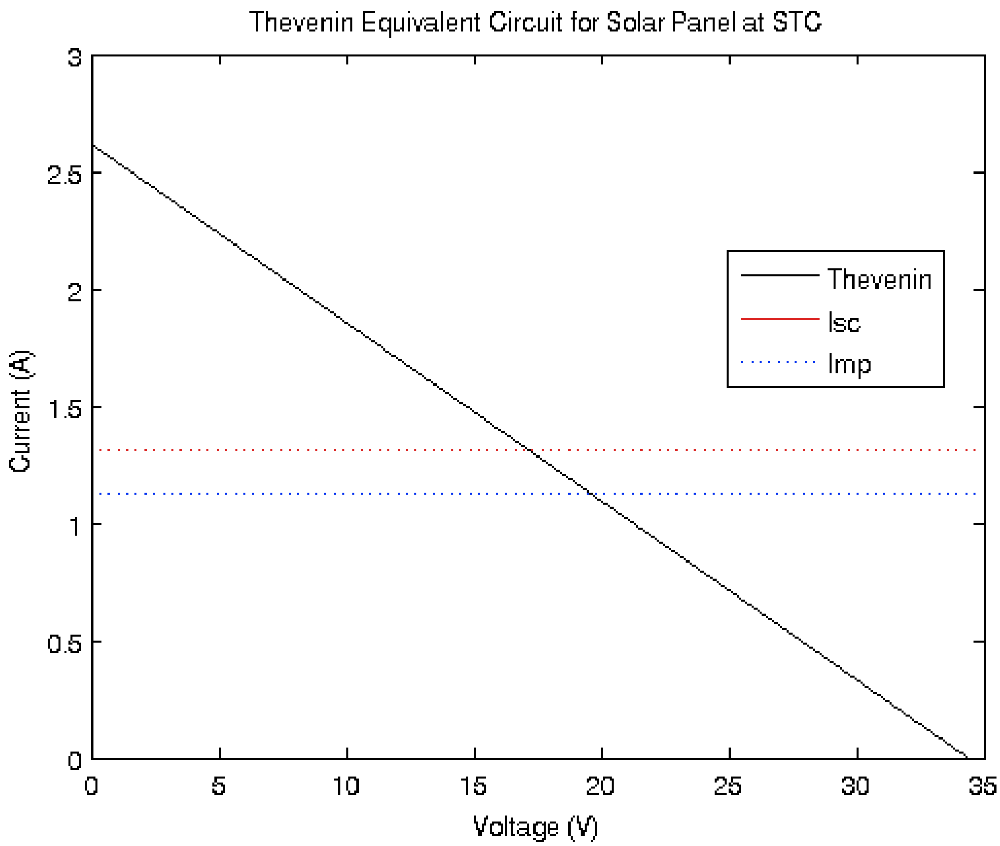

Figure 14: Graph of Thévenin voltage source for the solar panel.

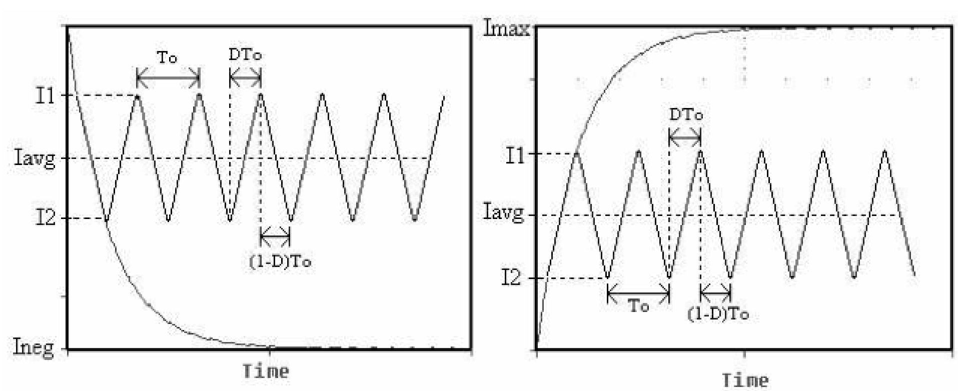

Figure 15: Graph of current through inductor for a high-frequency driver. Credit for image in [7].

$$I(t) = I_f - (I_f - I_i)e^{\frac{-t}{\tau}}$$
$$I(DT_0) = I_{max} - (I_{max} - I_2)(1 + \frac{-DT_0}{\tau})$$

$$I_1 = I_{max}(\frac{DT_0}{\tau}) + I_2(1 - \frac{DT_0}{\tau}) \tag{5}$$

A similar analysis for when the switch opens gives us an expression for I_2:

$$I_2 = I_{neg}(\frac{(1-D)T_0}{\tau}) + I_1(1 - (\frac{(1-D)T_0}{\tau})) \tag{6}$$

Now we can derive an expression for I_{avg}, the average current.

$$I_{avg} = \frac{I_1 + I_2}{2}$$

Again applying the assumption that $DT_0 << \tau$, we have

$$I_{avg} = I_{max}D + I_{neg}(1 - D) \tag{7}$$

From (7) we see that the average current should increase as the duty cycle increases. Similar analyses can be performed to find V_{avg} and from there, P_{avg}, R_{eq} and the voltage and current ripple. Their derivations are omitted here.

4.8 Microcontroller

The switch in the circuit will be controlled by a microcontroller. Specifically, the microcontroller will output a pulse-width modulated (PWM) signal. The microcontroller also possesses onboard analog-to-digital converters and math functions which will be needed to calculate the instantaneous power.

The controller being used in this application is an Atmel ATTiny25. It is built on an AVR architecture and has a maximum operating frequency of 1 MHz.

4.9 MOSFET selection

Now that we have electrically characterized the buck converter, we can select the physical parts from which to build it. The first part that is needed is a PMOSFET to do the switching. It is important that this device be as efficient as possible, so we will select a MOSFET based on power consumption.

There are three sources of power loss in a MOSFET: the on-state resistance $r_{ds,on}$, the gate charge Q_g, and the rise and fall times.

The equations for power absorbed due to each are given below:

$$P_r = I^2 r_{ds,on} \tag{8}$$
$$P_q = Q_g V_{gs} f \tag{9}$$
$$P_{rise,fall} = \frac{1}{2}(t_{rise} + t_{fall})V_{ds} \tag{10}$$

The first two equations are straightforward. The third equation is illustrated by Fig. 16. When a MOSFET is fully off, there is a voltage, V_{ds}, across it, but no current so the power absorbed is zero. When a MOSFET is fully on, there is a current through it but no voltage drop (save for that caused by the on-resistance) so again there is no additional power loss. But the switching time between on and off is not zero, so there are time periods where the current and voltage are both nonzero. We assume that the rise and fall of voltage and current happen right after another to simplify calculations to the simple geometry shown in Fig. 16.

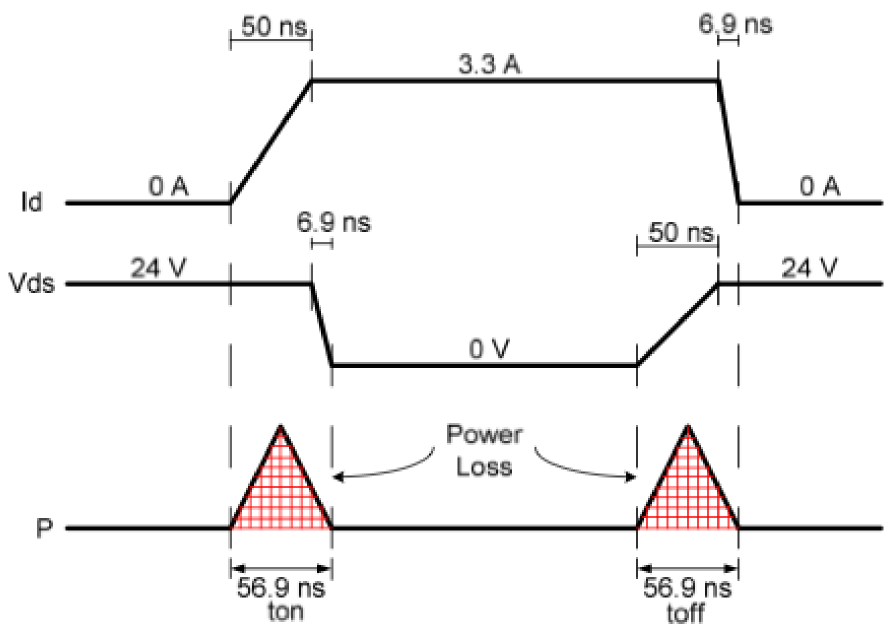

Figure 16: Illustration of power loss due to nonzero rise and fall times in a MOSFET.

Four candidate MOSFETs were analyzed with these equations. A graph showing power absorbed as a function of frequency is shown in Fig. 17. Based on this, we chose to use the FQP47P06 from Fairchild Semiconductor. The MOSFET will be driven at a frequency of 4 kHz, so this is well within this MOSFET's acceptable range.

The selection of inductor and diode were based mostly on simulation. The circuit was simulated in LTSpice and the peak current read from the simulation results. An inductance of 100μH yielded a good balance between current ripple and response. Selection of the 1N5404 diode was also based on simulation results. It is an inexpensive part and can pass up to 3 A.

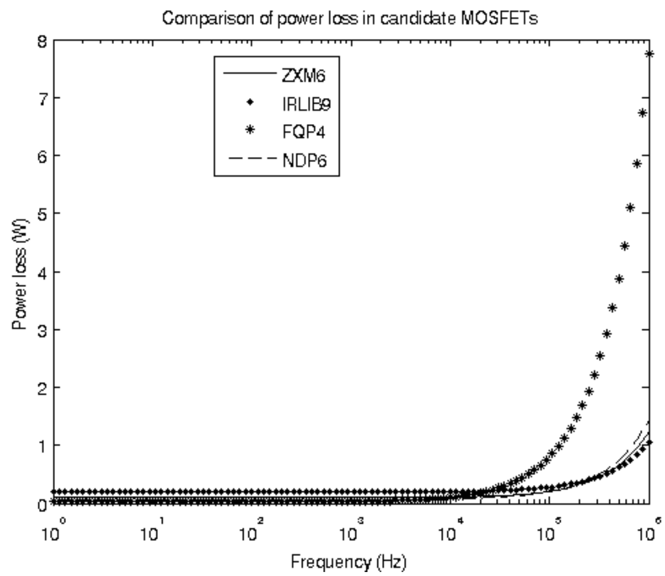

Figure 17: Power consumption analysis of four candidate MOSFETs. Note how certain MOSFETs are more desirable at lower frequencies, and quickly consume more power at higher frequencies.

4.10 Voltage and current sensing

In order to obtain the instantaneous power output from the solar panel we needed to measure the current and voltage. The ATTiny25 has three available ADC inputs. The maximum input voltage to any of the ADC channels is the supply voltage for the microprocessor, so a $\frac{1}{5}$ voltage divider was used to sample the voltage because the maximum voltage that could appear is $V_{oc} = 21.6$ V.

A current-sense resistor ($1\ \Omega, 1\%$ tolerance) was used to estimate the current output. According to Ohm's law, the voltage drop across the resistor is proportional to the current flowing through it. Another $\frac{1}{5}$ voltage divider was used to sample the voltage on the cathode of the resistor. See Fig. 18.

4.11 Program structure

The "tracking" of the maximum power point is the responsibility of the ATTiny25 program. The program samples its ADCs to arrive at a voltage and current measurement with ten-bit resolution. The program multiplies these together to arrive at a power estimate, which is stored in memory. The program then uses a "perturb and observe" strategy to find the maximum power point. On the first execution of the program, it arbitrarily decides to go "up" on the I-V curve; that is, to increase the duty cycle of the PWM output to the MOSFET switch so that more current is passed to the output.

The program loops and takes another measurement. If the power value was greater than the previous value, then the program knows it is on the "right track", approaching the maximum power point, and continues to go in the same direction: either increasing or decreasing the duty cycle. If the current power value was less than the previous, then the program reverses directions. This

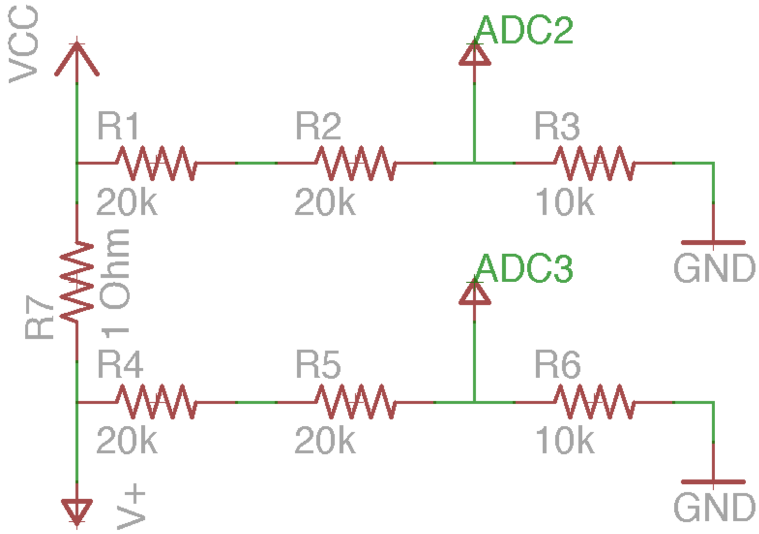

Figure 18: Voltage dividers used in voltage and current sampling by the ATTiny25.

loop continues indefinitely. The result is a real-time response to the changes in input power to the system.

The C code is given in the Appendix.

5 Results and discussion

The circuit was built according to the schematic in Fig. 9 and with the parts identified in the previous section. A power supply to simulate the solar panel was connected to the input and the output current was measured as a function of duty cycle (hardcoded in the program, as opposed to the dynamic response as discussed in the previous section). The results are shown in Fig. 19.

As can be seen, the average output current increased with duty cycle, verifying the operation of the buck converter. Measurements were taken until the solar panel short-circuit current was reached; this is the practical limit to the system, so no more measurements were taken. There is a large difference between the simulated values and the experimental values. This is due to the negative saturation current in the model equations. The diode actually prevents the current from becoming negative, but the current still decreases *as if* it were going to get to I_{neg}. In the future, it would be helpful to create a model which takes the diode negative current blockage into account.

Another interesting result was taken from the current-sense resistor. An oscilloscope trace of the voltage across the resistor as a function of time is given in Fig. 20. The lower trace shows the voltage as being input to the second ADC for determining the current. The important thing to note is that the voltage value is saturating instead of switching as was assumed would happen in Fig. 15.

This indicates that the buck converter is operating in *discontinuous mode*, which means that on every switching event the current and voltage are saturating to their minimum values. This result

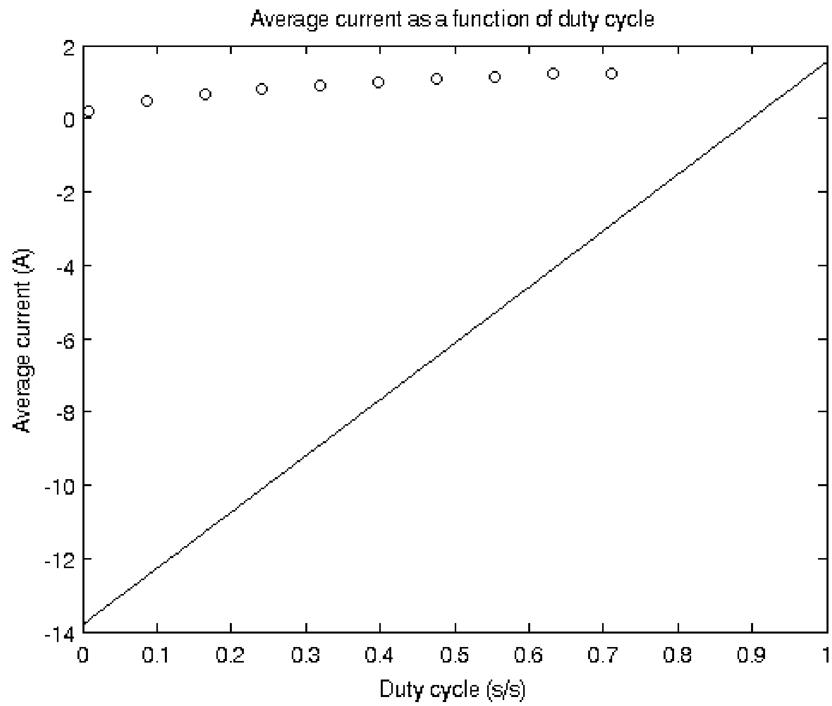

Figure 19: Average current through the inductor according to model equation and experimental results. The average current increases with increased duty cycle as expected.

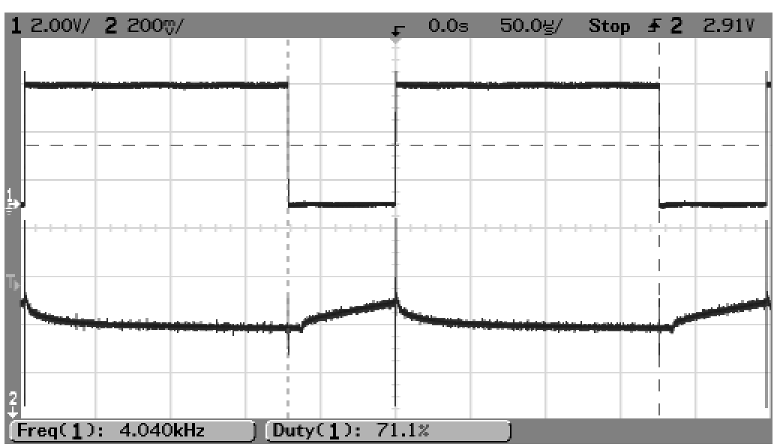

Figure 20: Trace 2 shows that the MPPT is operating in discontinuous mode.

is confirmed by simulation results. See Fig. 21.

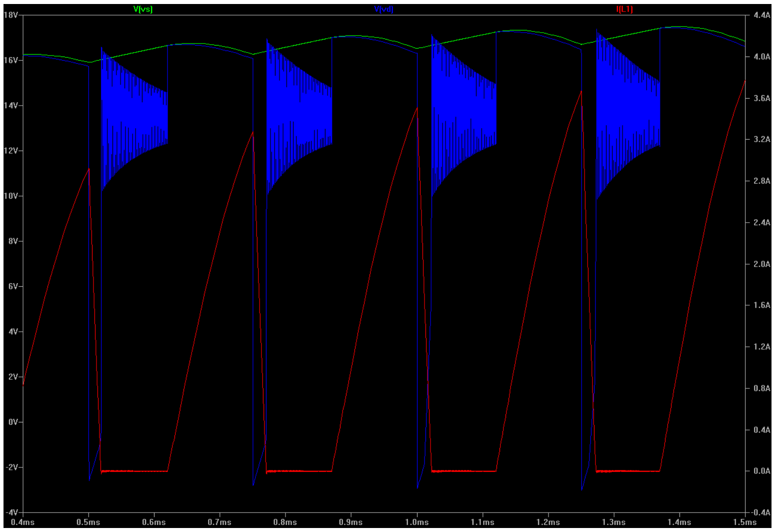

Figure 21: Simulation results that show the buck converter is operating in discontinuous mode.

In order to keep the ripple on I_{avg} to a minimum, the buck converter should be operated in continuous mode. This means that the operating frequency of the system needs to be increased. The problem with this is that the ATTiny25 may no longer be able to be used. The PWM output mode used to alter the duty cycle disallows changes to the output frequency.

Another output mode can be used to change the frequency, but in this case the duty cycle will remain constant, which prevents changing the operating point of the solar panel. Larger AVR microcontrollers exist to which the code could easily be ported. These microcontrollers usually have higher operating frequencies.

If the frequency were increased, then this would change other circuit components as well. The MOSFET may have to be changed due to the rapid increase in power dissipation of the current MOSFET for high frequencies. Other parts could be made smaller, further decreasing the total power dissipation in the circuit.

There is more room for improvement. In what is called a "synchronous buck" DC-DC switched power supply, the flywheel diode is replaced by another MOSFET switch. This eliminates the power loss across the diode when it is conducting ($V_F = 0.7$ V for Si diodes). A NMOSFET with its gate tied to ground is needed. See Fig. 22.

This model was simulated. The results are shown in Fig. 23. The current does not drop below zero, but voltage spikes due to the inductor may call for very specific components to be used.

Translating this design to the PCB would also decrease the input noise for the ADCs, leading to more accurate sampling. Currently, the PWM tends to oscillate around the MPPT. This is due to about ripple noise on the input to the ADCs. Much of this is due to capacitive coupling with high-frequency traces on the protoboard. Proper use of ground planes and layout of the PCB can greatly decrease this coupling noise.

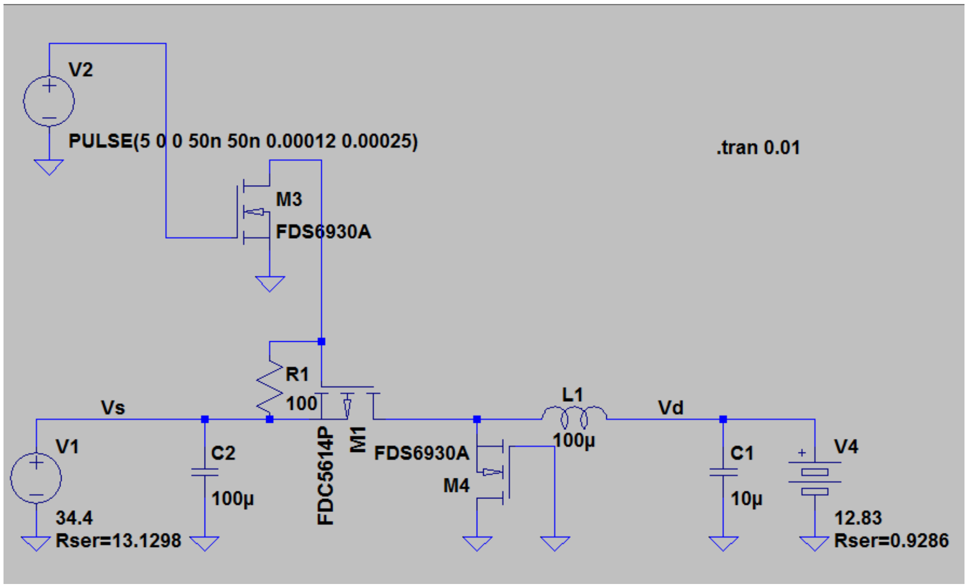

Figure 22: Maximum power point tracker with synchronous switching to avoid power losses through the freewheel diode.

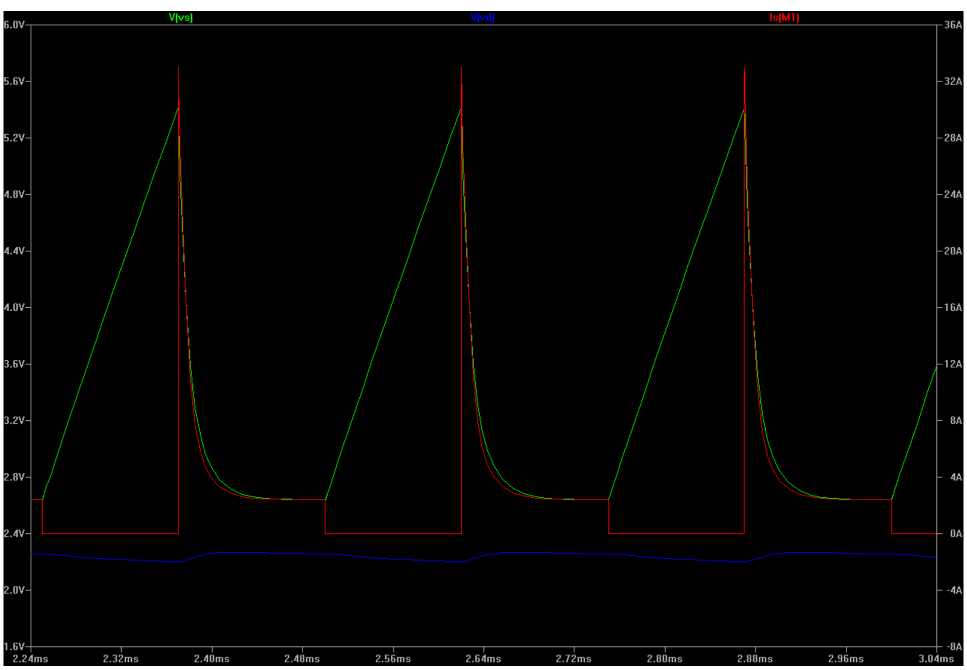

Figure 23: LTSpice simulation showing operation of synchronous buck converter.

6 Village Energy business model

Village Energy (U), Ltd., the startup company with which we partnered for this project, has a unique position among its competitors because it seeks to directly impact the value of the home, rather than to provide a tool such as a lantern. Installing lights in the home has a different effect on a homeowner than owning a flashlight, no matter how powerful the flashlight is.

The ability to flip a switch and have lights come on is a first-world privilege and certainly evidence for breaking into the 500 kWh club. The idea behind the current system is to create a "base" system consisting of a 20 W solar panel, a SLA battery, an MPPT with battery protection code, lights and a radio.

This would be the basic system that new users would purchase. Then, once they have made more income from the increased productivity that the lighting system afforded them, they would be able to easily install a new upgrade: a television or a refrigerator, for example. 12 V models for these appliances exist and are easily integrated into the base system. The idea is to have multiple ports available on the base station that any of the "upgrades" would be able to fit into. Having the system be able to work with the new upgrade is as easy as installing new software on the microcontroller chip, which is easily performed by Village Energy technicians.

Reflecting on the diffusion curve, it is not difficult to believe that diffusion rates will increase after an initial purchase of a Village Energy home system. Users will be familiar with the system and purchasing upgrades is not as risky as investing in a completely new product, as what might be the case in buying these appliances from other suppliers. Other suppliers' products may also not work with the solar panel.

Village Energy has a guarantee that all products will work with the system, preventing any of this hassle. They also have guarantees on customer service, honoring a two-year warranty on the system for any defects or mistakes in installation.

Village Energy has adopted a franchise model for selling the systems. From headquarters in Ntinda, Uganda, the parts are distributed to regional and local dealers. These dealers purchase the systems from headquarters and it is their responsibility to line up customers and to carry out the installation by contracting out electricians. To prevent extensive overhead at headquarters, these dealers are also in charge of customer service. It is no surprise that these dealers must be trained extensively at headquarters to keep the company's reputation in good standing.

Village Energy already has dealers in many parts of southeastern Uganda and is expanding into new areas every day, most notably looking at franchises in Kenya and the DRC.

7 Thematic coherence

The goal of the Grand Challenges Scholars program is to create pragmatic research projects that can be directly applied to the real world. In this section, we will analyze this project with respect to each of the five "pillars" of a Grand Challenges Scholars research project, both individually and together, as they relate to the NAE Grand Challenge of making solar energy economical.

The first pillar of the Grand Challenges Scholar project distinction is in-depth research. In this case, this component is self explanatory; three semesters of research have yielded two prototypes: one, an inexpensive circuit for regulating battery charge state, and another for getting the most value out of a solar panel by constantly transferring maximum power from the solar panel to the battery. Although these outcomes are oriented more towards product development than pure science, they still used math and science concepts to improve on an existing design. Theoretical models were compared to experimental results and correlated well.

The second pillar is interdisciplinary curriculum. The analysis skills needed to make the design decisions used in this class came from a variety of classes. Naturally, much was learned from electrical engineering courses in microelectronics; however, courses in computer science also aided in program design and understanding the AVR architecture. A house course, however, was equally important: "Technology and International Development." In this class, which was taught by students, the researcher learned about diffusion curves and what makes truly transformational products successful and why. The approach of creating a design that can reach, on a basic level, most potential clients and also offers easy upgrade options comes from this course.

The third pillar is entrepreneurship. This NAE Grand Challenges is especially suited for entrepreneurial approaches because it deals with making something "economical", which, as we discussed in the beginning of this paper, is intimately intertwined with issues of customer access and customer satisfaction. For this particular project we have actually partnered with a real entrepreneurial venture whose vision it is to eliminate electricity disenfranchisement and the dangers of using kerosene. This is perhaps the most powerful aspect of the project because it grounds it in reality. Already the research innovation is being tested and applied in the field. The difference that the Grand Challenges Scholars program has over other research programs is this deliberately pragmatic approach which requires researchers to think not only about the research, but also about how the research will be applied. This application aspect is manifested most clearly in a business model.

The fourth pillar is global perspective. Living for two months in Uganda for the Village Energy internship showed the researcher firsthand the conditions that prevail in areas that are untouched by the grid. Being able to put oneself in the shoes of the client illuminated exactly what the "experience" of living without electricity was, and what was most needed. This translated directly into business and design ideas for the next revision of the solar home system.

The final pillar of the Grand Challenges Scholars portfolio is service learning. Throughout this semester, the researcher worked with a student from the North Carolina School of Science and Math (NCSSM) named Grant Means. Grant was helpful in brainstorming new ideas for the project and performing some of the analysis, but more importantly he was a liaison to the school. We are in the process of creating an organization that will focus on creating solar projects, hopefully culminating in several highly visible installations on the campus grounds. This will sensitize others to the potential of solar power and attract other designers to the cause. This "pay it forward" aspect is perhaps the most important component because it educates the next generation to care about these issues and to start releasing their creative powers towards solving them. That is the key to solving the Grand Challenges.

8 Conclusion

Small-scale solar systems have the potential to instantly change the way the bottom of the pyramid lives. Decentralized home systems don't depend on unreliable grid systems, if they exist at all. They are built from components that are becoming more and more accessible from a price and inventory perspective. The addition of just 500 kWh has been shown to greatly impact HDI.

We have designed a system that provides the basic protections to the battery and that searches for the maximum power point of a solar panel under changing insolation conditions. Currently, this design is still being prototyped, but once it is finished it will be manufactured and distributed by Village Energy (U), Ltd., a startup company in Uganda. Through this effort, and through an educational program started at NCSSM, we rapidly approach an economical solar power solution.

9 Appendix

```
/*
 * main.c
 *
 * Device implementation of maximum power point tracker
 * and charge controller for home solar systems.
 *
 * @author Eric Thorne
 */

#include <stdlib.h>
#include <avr/io.h>
#include <avr/interrupt.h>
#include <util/delay.h>

volatile char adc_flag = 0;

/*
 * initPWM
 *
 * configures the AVR device to use the PWM component correctly
 */
void initPWM() {
	OCR0A = 180;
	TCCR0A |= (1 << COM0A1); // clear OC0A on compare match
	TCCR0A |= ((1 << WGM00) | (1 << WGM01)); // fast pwm mode, count from BOTTOM (0x00)
	TCCR0B |= (1 << CS00); // clock = clock_io
	DDRB |= (1 << 0); // configure OC0A as an output
}

/*
 * initADC
 *
 * configues the AVR devices to use the ADC component correctly
 */
void initADC() {
	ADCSRA |= (1 << ADEN); // enable adc; this allows other options to be set
	// do not change reference; default is OK (vcc)
	ADCSRA |= ((1 << ADIE) | (1 << ADPS1) | (1 << ADPS0)); // 125 khz prescaler
	ADMUX |= (1 << MUX1) | (1 << MUX0); // set to current at first, will be toggled
	ADCSRA |= (1 << ADSC); // throw out first conversion
	while (adc_flag == 0);
	adc_flag = 0;
}
```

```c

/*
 * runADC
 *
 * run a single conversion from the ADC
 */
void runADC() {
        // toggle the channel and run the adc
        ADMUX ^= (1 << MUX0);
        ADCSRA |= (1 << ADSC);
}

/*
 * calcPP
 *
 * calculates the current power point of the solar panel
 */
unsigned int calcPP() {
        runADC();
        while (adc_flag == 0);
        adc_flag = 0;
        int voltage = ADCL;
        voltage += (ADCH << 8);
        runADC();
        while (adc_flag == 0);
        adc_flag = 0;
        int current = ADCL;
        current += (ADCH << 8);
        unsigned int power = voltage*(voltage - current);
        return power;
}

/*
 * upDuty
 *
 * increase PWM frequency by a constant quantum
 */
void upDuty() {
        if (OCR0A < 255) {
                OCR0A++;
        }
}

/*
 * downDuty
```

```c
 *
 * decrease PWM frequency by a constant quantum
 */
void downDuty() {
        if (OCR0A > 1) {
                OCR0A--;
        }
}

int main() {
        unsigned int power, lastPower;
        sei(); // enable global interrupts
        PRR |= (1 << PRTIM1); // disable timer/counter 1
        initPWM();
        initADC();
        lastPower = calcPP();
        upDuty(); // arbitrarily try going up
        char dir = 1;
        while (1) {
                power = calcPP();
                if (power > lastPower) { // power increased, keep on going in same direction
                        if (dir == 1) {
                                upDuty();
                        } else {
                                downDuty();
                        }
                } else if (power < lastPower) { // power decreased, reverse directions
                        if (dir == 1) {
                                downDuty();
                                dir = 0;
                        } else {
                                upDuty();
                                dir = 1;
                        }
                }
                lastPower = power;
                // if power was the same, then don't adjust (we should have a tolerance on t
                // to be calculated from thevenin model so that we don't adjust too often
        }
        return 0;
}

ISR (ADC_vect) {
        adc_flag = 1;
}
```

10 Works cited

1: Statistical Review of World Energy 2009, BP. July 31, 2006.
2: Smil, V. 1991. General Energetics Energy in the Biosphere and Civilization. John Wiley, New York.
3: National Academy of Engineering. "Make solar energy economical."
4: Rogers, E. M. *Elements of Diffusion.* 5th ed. August 16, 2003.
5: Leung, Chi Seng and Meisen, Peter. "How electricity consumption affects social and economic development by comparing low, medium and high human development countries." GENI. 2005.
6: Pasternak, A. D. "Global Energy Futures and Human Development: A Framework for Analysis." US DOE: Lawrence Livermore National Laboratory. 2000.
7: Anderson, E., Dohan, C., and Sikora, A. "Solar Panel Peak Power Tracking System". Worcester Polytechnic Institute. March 12, 2003.
8: Chin, S., Gadson, J., and Nordstrom, K. "Maximum Power Point Tracker." Tufts University Department of Electrical and Computer Engineering. May 12, 2003.
9: Koutroulis, E., et al. "Development of a Microcontroller-Based, Photovoltaic Maximum Power Point Tracking Control System". IEEE Transactions on Power Electronics, Vol. 16, No. 1, January 2001.
10: Pandey, A. et. al. "Design Issues in Implementing MPPT for Improved Tracking and Dynamic Performance". IEEE.